Effect of pH and Concentration on Column Dynamics of Weak Electrolyte Ion Exchange

Marcel L. Jansen, Gerard W. Hofland, Joop Houwers, Adrie J. J. Straathof, Luuk A. M. van der Wielen, Karel Ch. A. M. Luyben, and Will J. J. van den Tweel
Dept. of Biochemical Engineering, Delft University of Technology, Julianalaan 67, 2628 BC Delft, The Netherlands

The column dynamics of simple ion-exchange processes involving acetic acid and N-acetylmethionine were studied using a strong-base anion exchange resin to reveal the complex relation between pH, concentration, equilibrium isotherms, and chromatographic separation in ion-exchange chromatography of weak electrolytes. Changing either the influent pH or the concentration, while keeping the other variable constant, led to considerable effluent concentration and pH fluctuations, respectively. This behavior is caused mainly by the uptake of undissociated acids. To describe these phenomena quantitatively, a rigorous thermodynamics-based equilibrium model for ion exchange, including Donnan potential and reaction equilibria, was incorporated into a fixed-bed model. Experimental results can be described well by this dynamic model, which is superior to conventional models due to its explicit incorporation of coions and partitioning of neutral species. It has great potential for optimizing chromatographic separations of weak electrolyte solutions.

Introduction

Ion-exchange processes of weak electrolytes are complicated by the fact that weak electrolytes occur in various pH-dependent, ionic states. Usually the strength of the interaction with the ion-exchange resin varies with different components. For weak electrolytes, differences also exist in the interaction of various ionic forms of a single component with the resin. In general, the uptake of counterions and the Donnan exclusion of coions by an ion-exchange resin are stronger as the valence of the ion increases (Helfferich, 1962). These electrostatic interactions between ions and the functional groups of the resin are much stronger than those of uncharged species that may occur in solutions of weak electrolytes as well. The liquid-phase pH that determines which ionic form of a weak electrolyte dominates is therefore a crucial factor in the retention of weak electrolytes on ion-exchange columns.

Correspondence concerning this article should be addressed to L. A. M. van der Wielen.
Current address of W. J. J. van den Tweel, DSM Andeno, P.O. Box 81, 5900 AB Venlo, The Netherlands.

Sorption of neutral species

The exchange of ions is usually described by stoichiometric models, with selectivities between ions as the major parameters (Helfferich, 1962). There is, however, less consensus about the uptake of neutral or zwitterionic species. Often sorption of these species has not been considered explicitly in ion-exchange models (Myers and Byington, 1986; Jones and Carta, 1993a). In other cases, they have been assumed not to be absorbed by the resin, although their presence is recognized (Helfferich and Bennett, 1984a,b; Saunders et al., 1989). However, the uptake of neutral species has already been demonstrated unarguably by Reichenberg and Wall (1956), who observed a considerable uptake of weak acids, such as acetic, propionic, and benzoic acid, by cation-exchange resins. Anions cannot be exchanged by such resins so the uptake must have concerned the neutral acid molecule. In models that allow for the uptake of the neutral species, the uptake has been related to the exchangeable counterion via the acid/base dissociation equilibrium (Kawakita and Matsuishi, 1991) or to the ionization constant of incompletely ionizing salts (Mehablia et al., 1994). Yu et al. (1987) described the

uptake of the net neutral, zwitterionic species of amino acids on a cation-exchange resin in a similar manner as that of the cationic species, i.e., with a selectivity parameter. Helfferich (1990) assumed a linear uptake isotherm for neutral species. Recent work by Jansen et al. (1996a) and also experiments by Reichenberg and Wall (1956), demonstrating a fairly linear behavior up to concentrations of 2 mol/L, support the assumption of linear uptake.

Objective

This article focuses on the chromatographic behavior of the weak acids *N*-acetylmethionine and acetic acid. These components are the substrate and the side product in the industrial enzymatic production of enantiomerically pure L-methionine from *N*-acetyl-DL-methionine (Wandrey and Flaschel, 1979; Chibata and Tosa, 1976), and therefore their separation is of considerable commercial interest. Both components are weak acids with different pK_a values, 3.52 for *N*-acetylmethionine and 4.76 for acetic acid. Therefore, the pH is a key variable that determines the difference in the degree of dissociation of the two components. The relative amounts at which the anionic and neutral forms of these components occur determine the extent each of the species is taken up. Moreover, there seems to be an interaction between the concentration and the pH: in single-component experiments with acetic acid/acetate Helfferich found considerable and prolonged pH excursions when the influent concentration of an anion-exchange column was changed while the pH was kept constant (Helfferich and Bennett, 1984a; Bennett and Helfferich, 1984). In comparable preliminary experiments with either acetate or *N*-acetylmethionine or both acetate and *N*-acetylmethionine, we observed similar phenomena that could not be described with traditional models.

The objective of this study is to investigate and describe the complex role of the pH and the concentration of acetic acid and *N*-acetylmethionine on their equilibrium uptake by a strong-base anion-exchange resin in ion-exchange chromatography, with special emphasis on the role of neutral species. This enables the design of an ion-exchange chromatography process for these two components in particular, and for weak electrolyte mixtures in general. The importance of pH and concentration on the equilibrium uptake has already been shown by means of batch equilibrium experiments using the Donnan Ion eXchange (DIX) equilibrium model (Jansen et al., 1996a). Since chromatography of small solutes is largely local-equilibrium-controlled, we have used a local-equilibrium fixed-bed model based on the DIX model to describe the dynamic behavior of ion-exchange columns. In this article the attention is focused on systems containing a single weak electrolyte. Multicomponent systems will be presented later (Jansen et al., 1996b).

Theory

Traditional models

Traditional ion-exchange models, such as the stoichiometric displacement model, predict stoichiometric exchange of ions based on the mass action law, with a maximum adsorption that is determined by the resin capacity (Helfferich, 1962; Jansen et al., 1996a). Extension of the model by taking the uptake of compounds in the pore liquid into account (Bellot and Condoret, 1991) improves the description of the dynamic behavior only to a limited extent because in this description the pore liquid is an integral part of the mobile phase. The uptake according to this nonstoichiometric sorption model is described by the following equation for univalent ions

$$c_i^R = Q \cdot \frac{c_i^L S_{i,j}}{\sum_{i=1}^{n} c_i^L S_{i,j}} + \epsilon_p c_i^L \tag{1}$$

Here Q is the resin capacity ($mol \cdot m^{-3}$) based on the hydrated resin volume, c_i is the concentration ($mol \cdot m^{-3}$) of ion i, $S_{i,j}$ is the selectivity of ion i over j and ϵ_p is the volume fraction ($m^3 \cdot m^{-3}$) of liquid-filled pores in the resin particle. Index R denotes the resin phase, index L the liquid phase and n is the total number of different counterions. The selectivity between univalent ions i and j is defined as

$$S_{i,j} = \frac{c_i^R}{c_i^L} \frac{c_j^L}{c_j^R} \tag{2}$$

Taking the adsorption of acetic acid on an anion-exchange resin as an example, this model predicts that the resin is completely in the acetate form over a wide concentration and pH range. At both low and medium pH, the OH^- concentration is completely negligible compared to the acetate concentration. Therefore, a chromatographic model on this basis predicts that moderate variations in the influent concentration or pH of an ion-exchange column would lead to a practically unmodified profile in the effluent. However, experiments by Helfferich and Bennett (1984a) indicate differently. A changing influent concentration led to a change of the effluent pH. Although Helfferich and Bennett could predict the amplitude of this pH excursion, they were not able to predict the duration and shape of the response correctly. They ascribed this to the uptake of neutral species, which is not incorporated in traditional models.

Donnan ion-exchange equilibrium model

In this article the Donnan Ion eXchange model (Jansen et al., 1996a) is used for simulating the dynamic behavior of ion-exchange columns. The core of the equilibrium model is the equality of chemical potentials in the resin and liquid phase for all species present in the system. That includes counterions as well as coions and neutral species. In this way the following equation was derived for the resin-phase concentration of anion a using an anion-exchange resin in a system with univalent ions

$$c_a^R = c_a^L S_{a,OH^-} \frac{Q + \sqrt{Q^2 + 4AC}}{2A} \tag{3}$$

where A and C (auxiliary functions, $mol \cdot m^{-3}$) defined as

$$A = \left(\sum_a c_a^L S_{a,OH^-} \right) \quad C = \left(\sum_c c_c^L S_{c,H^+} \right) \tag{4}$$

Index c denotes cations, S_{a,OH^-} is the selectivity of anions over OH^-, and S_{c,H^+} is the selectivity of cations over H^+. All like ions can be related to each other through the selectivities (Eq. 2). The cation (coion) concentration is given by

$$c_c^R = c_c^L S_{c,H^+} \frac{2A}{Q + \sqrt{Q^2 + 4AC}} \tag{5}$$

The uptake of a neutral species i was shown to be proportional to the liquid phase concentration if the water concentration ratio between both phases is constant

$$c_i^R = c_i^L K_i^{ov} \tag{6}$$

where K_i^{ov} is the overall distribution constant. This is a function of standard chemical potentials $\Delta\mu^0$ and partial molar volumes $\bar{\nu}$ ($m^3 \cdot mol^{-1}$) of water (w) and species i

$$K_i^{ov} = \left(\frac{c_w^R}{c_w^L}\right)^{\frac{\bar{\nu}_i}{\bar{\nu}_w}} \cdot \exp\left(\frac{\left(\Delta\mu_w^0 \frac{\bar{\nu}_i}{\bar{\nu}_w} - \Delta\mu_i^0\right)}{RT}\right) \tag{7}$$

The total uptake of a component occurring in both anionic, cationic and/or neutral form is given by the sum of the contributions of Eqs. 3, 5 and 6.

Fixed-bed model

The differential mass balance equation for a fixed-bed ion-exchange column with plug flow and axial dispersion, dimensionless in space and time, reads

$$\frac{\partial c_i^L}{\partial\theta} + \frac{(1-\epsilon_b)}{\epsilon_b}\frac{\partial c_i^R}{\partial\theta} + \frac{\partial c_i^L}{\partial z} - \frac{1}{Pe}\frac{\partial^2 c_i^L}{\partial z^2} = 0 \tag{8}$$

Here θ is the dimensionless time, t/τ with τ the liquid residence time (s), ϵ_b is the void fraction of the bed and z is the dimensionless longitudinal coordinate, x/L, where L is the column length (m). Pe is the Peclet number defined as $u_0 L/\epsilon_b D_{ax}$, where u_0 is the superficial liquid velocity ($m \cdot s^{-1}$) and D_{ax} is the axial dispersion coefficient ($m^2 \cdot s^{-1}$). Assuming local equilibrium between resin phase and liquid phase while using the chain rule, the resin and liquid phase accumulation of component i are related through the following equation

$$\frac{\partial c_i^R}{\partial\theta} = \sum_{j=1}^{n} \frac{\partial c_i^R}{\partial c_j^L}\frac{\partial c_j^L}{\partial\theta} \tag{9}$$

Substitution of this equation into Eq. 8 while applying vector notation yields the following equation

$$(I_n + \beta\Gamma)\frac{\partial \underline{c}^L}{\partial\theta} + \frac{\partial \underline{c}^L}{\partial z} - \frac{1}{Pe}\frac{\partial^2 \underline{c}^L}{\partial z^2} = \underline{0} \tag{10}$$

Where I_n is the n-dimensional identity matrix, Γ is the Jacobian matrix of partial derivatives $\Gamma_{i,j} = \partial c_i^R/\partial c_j^L$, $\underline{c}$ is the vector of concentrations ($mol \cdot m^{-3}$), and β is the volume ratio of resin and liquid phase, $(1-\epsilon_b)/\epsilon_b$ ($m^3 \cdot m^{-3}$).

Numerical solution

The matrix of derivatives is determined numerically from Eqs. 3, 5 and 6 by calculating the change of the total resin phase concentration of the components after changing the liquid phase concentrations of each of the components by a finite quantity Δc, so $\Gamma_{i,j} \approx \Delta c_i^R/\Delta c_j^L$. The accompanying pH is calculated numerically by a hybrid Newton-Raphson method with the electroneutrality as a constraint.

If kinetic effects and dispersion are not negligible and the local equilibrium assumption is thus not valid, the kinetic effects and axial dispersion can be lumped into an apparent dispersion coefficient, D_{app}. The resulting model is known as the equilibrium-dispersive model (Golshan-Shirazi and Guiochon, 1992; Guiochon et al., 1994). The partial differential equations can be solved numerically by spatial discretization using finite differences (Carta et al., 1988; DeCarli II et al., 1990; Golshan-Shirazi and Guiochon, 1992; Guiochon et al., 1994). In this article backward spatial discretization will be used

$$\frac{\partial \underline{c}_k^L}{\partial z} = \frac{1}{\Delta z}(\underline{c}_k^L - \underline{c}_{k-1}^L) \tag{11}$$

Where $1/\Delta z$ equals the number of spatial discretization steps and index k denotes the kth discretization step. Following Guiochon and coworkers, the second-order term in Eq. 10 is eliminated. This is done by replacement of axial dispersion by numerical dispersion. For this purpose the proper number of discretization steps needs to be chosen. This leads to the following vectorial set of differential equations

$$\frac{\partial \underline{c}_k^L}{\partial\theta} = -\frac{1}{\Delta z}(I_n + \beta\Gamma)^{-1}(\underline{c}_k^L - \underline{c}_{k-1}^L) \tag{12}$$

These equations are integrated numerically using a fourth-order Runge-Kutta algorithm, written in Turbo Pascal 6.0 on a 486DX2 personal computer. The Courant-Friedrichs-Lewy convergence condition, required for a stable numerical solution, is given by Guiochon et al. (1994). Substitution of axial dispersion by numerical dispersion requires a proper choice of the number of discretization steps. The theoretical relations between actual and numerical dispersion were set up for linear systems. For nonlinear multicomponent systems, these are only approximate and should be used with care. Limited variations in the discretization step size often do not markedly affect the general characteristics of the simulation results (van der Wielen et al., 1993).

Materials and Methods

Chemicals

Acetic acid and sodium hydroxide (analytical grade) were obtained from Baker (Deventer, The Netherlands). *N*-acetyl-DL-methionine was obtained from Sigma (St. Louis, MO). Macro-Prep Q ion-exchange resin was obtained from Bio-Rad

(Hercules, CA). Macro-Prep Q is a macroporous, polyacrylate-based, hydrophilic, strong-base anion exchanger with quaternary ammonium functional groups. The resin characteristics have been determined previously (Jansen et al., 1996a).

Analyses

Off-line analyses of acetic acid and *N*-acetylmethionine (AcM) were done by HPLC on a Bio-Rad HPX-87H column of 7.8 mm ID and 30 cm length, operating at 60°C, with UV detection at 210 nm. The eluent was a 10-mM phosphoric acid solution of pH 2 at a flow rate of 0.6 mL/min. Acetic acid and *N*-acetylmethionine were also determined on-line from the UV absorption at 220 nm by simultaneous measurement of the pH and the pH-dependent UV absorption as described below.

Bed void fraction

The void fraction of the bed was determined by measuring the hydraulic residence time of inert tracers. The tracers used were methionine and arginine, which should be able to enter the resin due to their size, but the conditions of pH and concentration were chosen such that they were expelled effectively from the resin. At low pH both compounds are positively charged and exclusion of coions is virtually absolute in dilute systems (Helfferich, 1962). Therefore, a pulse of 10 mmol/L methionine at pH 2 with a duration of 5 s was given to a column of 21.2 mL, eluted with 10 mmol/L hydrochloric acid (pH 2) at a flow rate of 5.25 mL/min. An arginine pulse of 0.1 mmol/L at pH 4 was given during 30 s to a column of 21.7 mL, eluted with 0.1 mmol/L hydrochloric acid (pH 4) at a flow rate of 4.4 mL/min. The experiments were carried out at room temperature.

Acetate and N-acetylmethionine block-pulse in pH

Block-pulse experiments were carried out at room temperature using a fixed bed of Macro-Prep Q in a glass column of 1.5 cm ID with a precisely determined total bed volume of 20–25 mL. The column was equilibrated with an acetic acid or *N*-acetylmethionine solution of 100 mmol/L at a fixed pH and a flow rate of about 5 mL/min. After equilibration, the feed was changed to a solution of equal molarity but with a different pH and after the new equilibrium was reached for the entire column, the feed was changed back to the original solution and the column was equilibrated again. This procedure was repeated several times with solutions of different pH. A complete survey of experimental conditions is given in Table 1.

The effluent was analyzed on-line with a pH electrode with a 50-μL flow-through cell (model 5743900, Phoenix, Houston, TX) connected to a model 691 pH meter (Metrohm, Herisau, Switzerland), with a Ultrospec III spectrophotometer (Pharmacia LKB, Uppsala, Sweden) with variable wavelength, and with a Consort K720 conductivity meter (Consort, Turnhout, Belgium). Concentrations were calculated from the combination of UV absorption at 220 nm and pH, since the UV signal is pH-dependent because of a difference in absorption of the acid and conjugate base forms of acetic acid and of *N*-acetylmethionine. The on-line analyses were checked with off-line analyses.

Table 1. Experimental Conditions for pH Block-Pulse Experiments of Acetic Acid and *N*-Acetylmethionine

	Acetic Acid	*N*-Acetylmethionine
Column vol. (mL)	26.25	21.7
Flow rate (mL/min)	5.35	4.44
Conc. (mmol/L)	100	100
Reference pH	4.70	3.00
Other pH values	3.06, 4.00, 4.50, 5.50 6.50, 7.50, 9.10, 11	3.50, 3.96, 4.48, 5.00, 7.0

Acetate block-pulse in concentration

Concentration block-pulse experiments were done with a column of 26.25 mL at a flow rate of 5.4 mL/min. The bed was equilibrated with a solution of 10 mmol/L acetic acid at pH 4.75. Then the feed was changed to a solution of 100 mmol/L with the same pH. After equilibration, the feed was restored to the original solution. This procedure was repeated with solutions of pH 6.0.

Results and Discussion

Bed void fraction

A void fraction of 0.60 ± 0.03 was found with methionine as tracer and 0.60 ± 0.01 with arginine. This value does not correspond to a value of about 0.40, which is common for fixed beds with uniform spherical particles. Hence it may be concluded that a part of the intraparticle liquid, most likely the macropore fluid, actually belongs to the mobile phase and that the other part belongs to the stationary phase, probably the micropore fluid. The resin capacity was corrected for this effect; a value of 0.325 mol/L was used instead of the value of 0.217 mol/L presented previously (Jansen et al., 1996a).

Qualitative discussion of block-pulse of pH at fixed acetic acid concentration

The response of the column to a block-pulse in the pH from the reference pH of 4.70 to 7.50 and vice versa is shown in Figure 1. This type of response is characteristic for all block pulses of the influent pH. Despite the fact that the total acetate concentration in the influent was kept constant at 100 mmol/L, a 40–50% change of the effluent concentration was found in this experiment. This can only be due to a change of the equilibrium uptake. As indicated below, undissociated acetic acid is largely responsible for this.

The second striking effect is the very slow response of the pH to an upward pH step, much slower than expected on the basis of the hydraulic residence time, and the relatively fast response to a downward pH step. The reason for this is that the buffer capacity of a solution is maximal at a pH equal to the pK_a value, which is 4.76 for acetate. The introduction of an acetate solution with a higher buffer capacity in the downward pH step leads to a rapid increase of the H^+ concentration and decrease of the pH. For the upward step, on the other hand, the unbuffered solution at pH 7.5 is extremely sensitive to small quantities of H^+. The slow response can be attributed to the slow release of very small quantities of acetic acid due to very low concentration gradients.

The third feature of all experimental results is the appearance of a small shoulder at the onset of the pH response for

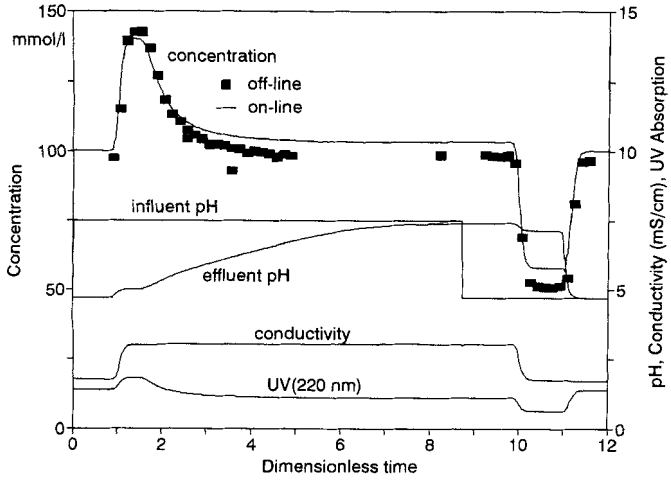

Figure 1. Response of a column in equilibrium with a 100 mmol/L acetate solution at pH 4.70 to a block pulse of 100 mmol/L acetate at pH 7.50.

both the upward and downward step. This shoulder, as can be seen in Figure 1, coincides with the rise and drop of the effluent concentration of total acetate. This can be explained using the wave velocity concept (Helfferich and Bennett, 1984a) for propagation of disturbances in the column. According to this theory the concentration velocity u_c of a non-reacting species i is given by the following relation

$$u_c = \frac{u_L}{1 + \beta\left(\dfrac{\partial c_i^R}{\partial c_i^L}\right)} \tag{13}$$

where u_L is the interstitial mobile phase velocity and the term $\partial c_i^R/\partial c_i^L$ represents the equilibrium isotherm. The introduction of a solution with a high pH results in an increase of the sodium concentration. Because most sodium cations are excluded by the resin due to the Donnan effect, the term $\partial c_{Na^+}^R/\partial c_{Na^+}^L$ will be small, and according to Eq. 13 a sodium wave will move through the column at approximately the mobile phase velocity. This explanation is supported by the rapid increase of the effluent conductivity after exactly one residence time, as shown in Figure 1. In order to maintain electroneutrality, the cations are accompanied by acetate anions, so this first wave is a combined Na^+/Ac^- wave.

According to Klein (1981), the number of waves is equal to the variance of the system, defined as the minimum number of concentration variables required to determine the composition of a system at equilibrium. This variance equals the number of variables minus the number of equilibrium equations and constraints. In this system the number of variables equals 10, namely, the concentration variables of Na^+, H^+, OH^-, Ac^- and HAc in both phases. Here, H is proton and HAc is acetic acid. The number of relations and constraints equals 8: water dissociation in both phases, acetic acid dissociation in the liquid phase, acetic acid distribution over resin and liquid phase, the selectivities between Ac^-/OH^- and Na^+/H^+, and electroneutrality in both phases. This means that a second wave is to be expected, just like in Helfferich's approach but without the assumption of total exclusion of coions and exclusion of neutral species. The second wave is linked with the uptake of undissociated acetic acid. The term $\partial c_{HAc}^R/\partial c_{HAc}^L$ in Eq. 13 is larger than zero and thus acetic acid migrates with a velocity smaller than the mobile phase velocity. The release (or uptake) of undissociated acetic acid leads to a disturbance of the dissociation equilibrium in the liquid phase. According to Van't Hoff's principle, this is counteracted by a redistribution of protons to restore the equilibrium which causes a temporary stabilization of the effluent pH. This continues until the new acetic acid distribution is established throughout the entire column and the second wave appears at the column outlet. Then both effluent pH and concentration change to their final (influent) values.

The general character of the above-mentioned phenomena for block pulses at other pH values is illustrated by the concentration profiles in Figure 2 and the pH profiles in Figure 3. It is clear from these figures that there is a relation between the pH, the total acetate uptake, and the occurrence of concentration waves. For the lower pH values, the velocity

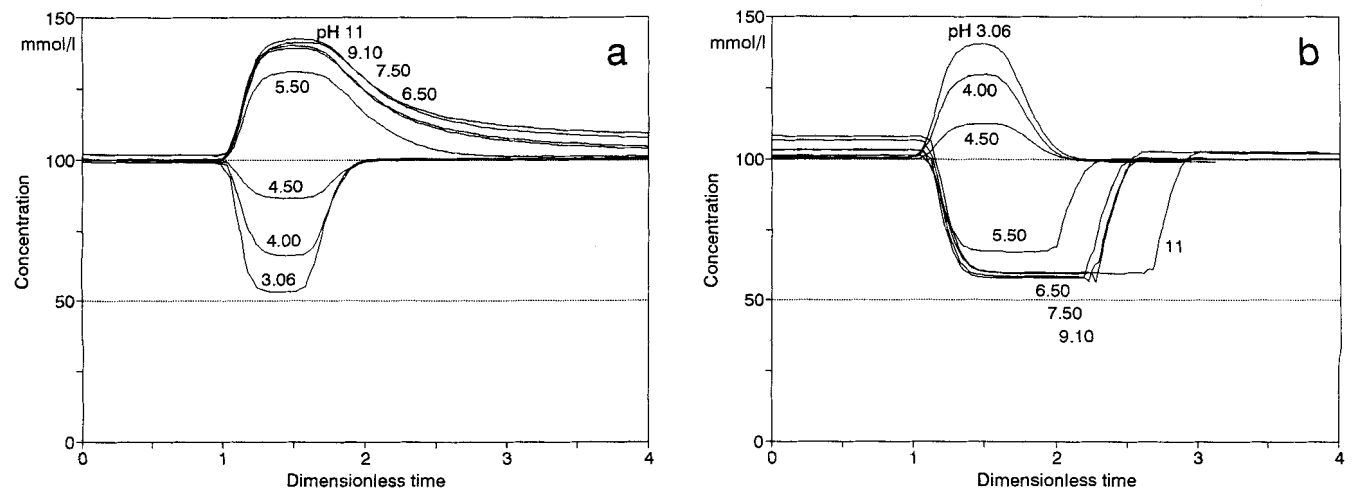

Figure 2. Effluent total acetic acid concentrations in response to block pulses of acetate solutions with different pH values at a constant feed concentration of 100 mmol/L.

(a) Block-pulse front; (b) block-pulse tail.

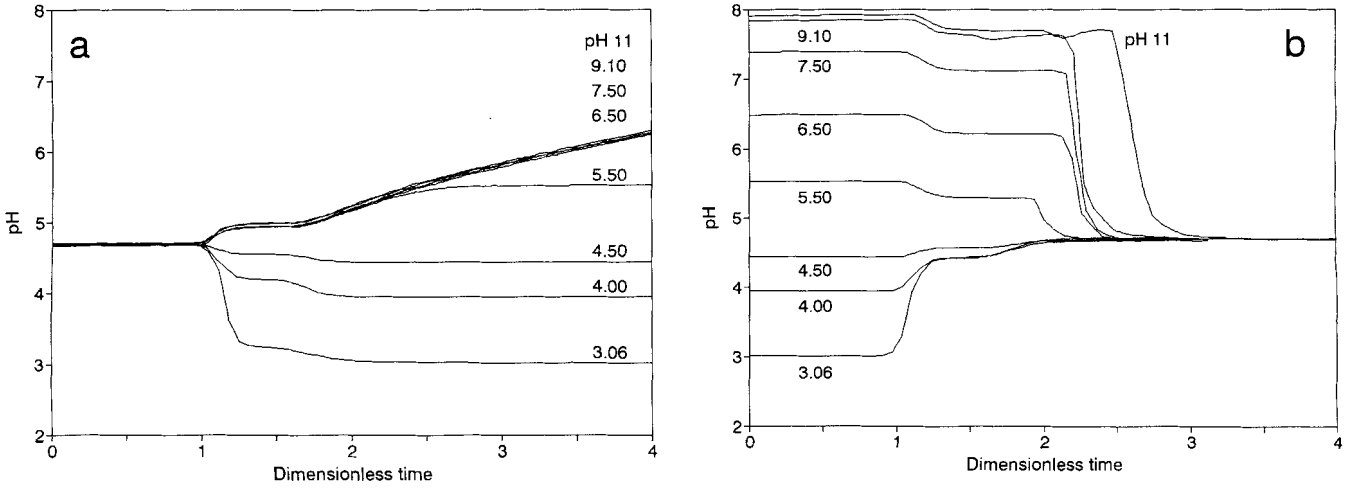

Figure 3. Effluent pH in response to block pulses of acetate solutions with different pH values at a constant feed concentration of 100 mmol/L.

(a) Block-pulse front; (b) block-pulse tail.

of the second wave, deduced from the width of the concentration fluctuations in Figure 2 and from the width of the pH plateaus in Figure 3, appears to be fairly constant. Only the amplitude changes. This means that the isotherm for neutral acetic acid is approximately linear and that the distribution coefficient $K_{\mathrm{HAc}} = \partial c^R_{\mathrm{HAc}}/\partial c^L_{\mathrm{HAc}}$ is approximately constant. Using Eq. 13 it follows from the location of the second wave at approximately 1.7 residence times that the distribution coefficient of acetic acid is close to unity. For higher pH values the distribution coefficient seems to have a higher value. The reason for this is not yet understood.

Determination of distribution coefficient of acetic acid

A quantitative picture of the acetic acid uptake is obtained by integrating the response of the acetate concentration in Figure 2. The uptake in excess to the uptake at the reference pH is calculated from these peak areas both for the front of the block-pulse and for the end of the pulse. The results of on-line and off-line analyses are in good agreement, but at higher pH some spreading occurs due to the very long times required to reach steady state.

In Figure 4 the excess uptake in comparison to that at the reference pH is plotted against the concentration of undissociated acetic acid. It follows that the excess uptake in comparison with the uptake at pH 7.5, where there is no undissociated acetic acid at all, is approximately 35% of the resin capacity at this particular feed concentration of 100 mmol/L. To determine the overall distribution coefficient, defined by Eq. 7, the results in Figure 4 were extrapolated to a concentration of undissociated acetic acid of 100 mmol/L. In that case the acetate anion and sodium cation concentrations approach zero. The term $4AC$ in Eq. 3 is then negligible and the resin phase acetate anion concentration becomes constant and equal to the capacity Q. A change in the undissociated acetic acid concentration in the liquid phase then leads to a proportional change of the resin phase acetic acid concentration. Hence, the overall distribution coefficient is equal to the slope of the curve in Figure 4 at the limit of the acetic acid concentration approaching 100 mmol/L. The value $K^{\mathrm{ov}}_{\mathrm{HAc}} = 0.90$ was obtained by fitting a linear distribution function through the data, using the measured bed void fraction of 60%. This corresponds to a wave location at 1.6 times the liquid residence time and is in good agreement with the results in Figures 2 and 3.

An alternative method to determine the distribution coefficient is to fit the DIX model through the data using a least-squares estimation procedure. Using only those data corresponding to a pH lower than the reference pH, for a more accurate estimation of the parameter, gave a value of 1.079. The use of this value in Eq. 13 indicates that the acetic acid wave is to be expected after 1.7 residence times, which corresponds well with the results in Figures 2 and 3.

From batch equilibrium studies values of 0.743 ± 0.063 and 0.876 ± 0.071 were found (Jansen et al., 1996a). Correction of these values for the fact that part of the intraparticle liquid

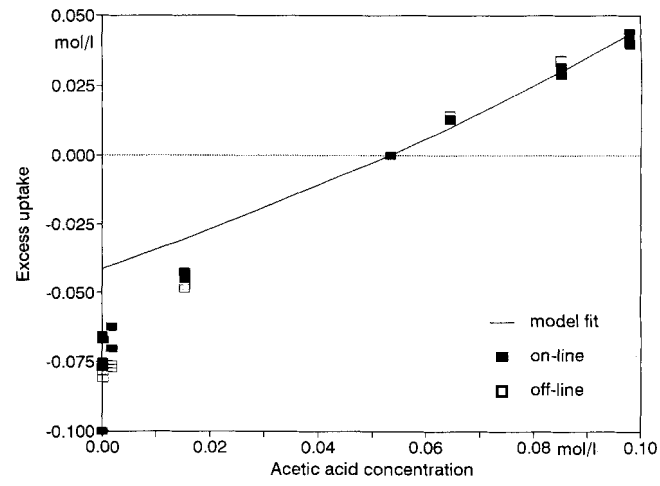

Figure 4. Excess resin-phase concentration of acetic acid and acetate as function of the undissociated acetic acid concentration relative to the acetate uptake at pH 4.70 at a constant feed concentration of 100 mmol/L.

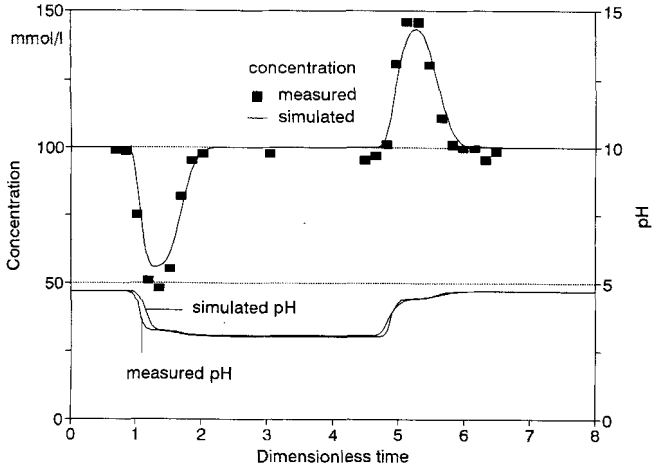

Figure 5. Experimental and simulated profiles of effluent concentration and pH for the acetate block pulse from pH 4.70 to pH 3.06 and *vice versa*.

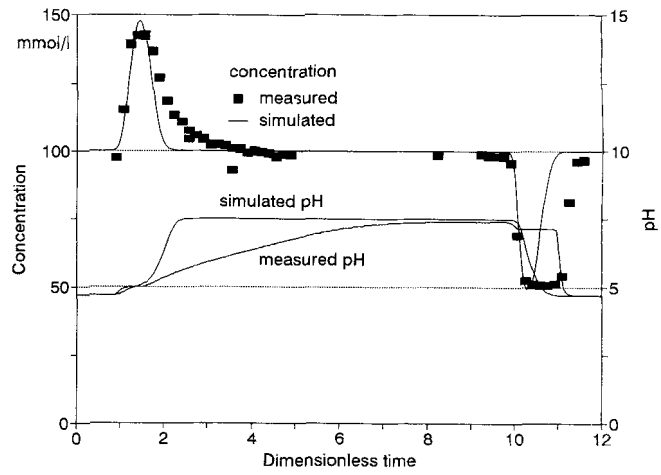

Figure 6. Experimental and simulated profiles of effluent concentration and pH for the acetate block pulse from pH 4.70 to pH 7.50 and *vice versa*.

belongs to the mobile phase, as stated above, gives an average value of 1.2 for the distribution coefficient. In view of the accuracy of these results, there is a good agreement with the results obtained in the present study.

Simulation of response to block-pulse of pH for acetate solutions

The response of the column to a block-pulse of the influent pH of the acetate solution was simulated using the model parameters given above: $\epsilon_b = 0.6$ and $K_{HAc}^{ov} = 1.079$, and those determined from batch experiments: $S_{Ac^-,OH^-} = 0.025$ and $S_{Na^+,H^+} = 28.7$ (Jansen et al., 1996a). It was demonstrated by analysis of characteristic times that the Peclet number was approximately 1,500 in all experiments (see Appendix), requiring 750 spatial discretization steps. However, intraparticle diffusion is not negligible—at the flow rates applied in this study the characteristic times for convective transport and diffusion are similar—and the apparent dispersion will increase and thus a lower number of discretization steps was chosen. The number of integration steps was adjusted to fit the steepness of the profiles. In general good results were obtained with 100 discretization steps. This number of steps was used throughout this work, unless stated otherwise.

Figure 5 shows that the simulations of pH and concentrations for the block-pulse of pH 3.06 are in excellent agreement with the experimental profiles. In this case the profiles are mainly determined by the magnitude of the overall distribution coefficient of the undissociated acid. The sensitivity for the other model parameters is very low. The quantitative agreement between simulations and experimental results in the case of pH 7.5 is less good (Figure 6). It is obvious from the concentration profile that the influence of the pH on the change of the total acetate uptake is underestimated by the model at higher pH values. This could be expected given the results in Figure 4. The disagreement in the pH profile is even more striking. The simulated front is sharper than expected and the tail is less sharp. Changing the number of discretization steps is not beneficial since it would sharpen (more steps) or flatten (less steps) the entire profile, and not just the front or end part. The reason for the measured slow response of the pH front is ascribed to mass-transfer inefficiencies. These cause a slow release of very small amounts of undissociated acetic acid to an unbuffered solution. Although this contributes little to the total acetic acid release, upon dissociation it produces a quantity of protons that is significant compared to the prevalent concentration of H^+, and this results in a serious lag in the pH. For the reverse step, the lag is absent due to the large buffer capacity of the influent. Lumping dispersion and kinetic and mass-transfer effects into a single apparent dispersion coefficient thus appears to be an oversimplification in case protons play such an important role.

Acetate concentration step experiments at constant influent pH

To check the validity of the DIX model as well as the dynamic simulation model and to investigate the general applicability for different ion-exchange resins, data from Helfferich and Bennett (1984a) were also used. These authors observed a marked fluctuation of the effluent pH after a change of the influent concentration of acetate solutions, fed to a fixed bed with the anion-exchange resin Amberlite IRA-400. The pH fluctuation was not only observed at high pH values, but even at pH values where the buffer strength of the acetate solutions is maximal, i.e., at pH values close to the pK_a value of acetic acid. The response of the pH to an upward concentration step from 0.1 mol/L acetate to 1 mol/L at pH 4.75 is shown in Figure 7a and the response to the reverse step in Figure 7b. The precise experimental conditions are given in the original article. Unfortunately, no information concerning the concentration profile is given. Although the ionic fraction of OH^- on the resin phase is already very low, the increase of the liquid phase acetate concentration further reduces this fraction. The released OH^- ions cause a temporary increase of the pH. The opposite happens when the concentration is reduced again.

The experiment was simulated with the value $S_{Ac^-,OH^-} = 2.95$, as given by the authors. The other parameter values were estimated and adjusted to fit the data. The optimal val-

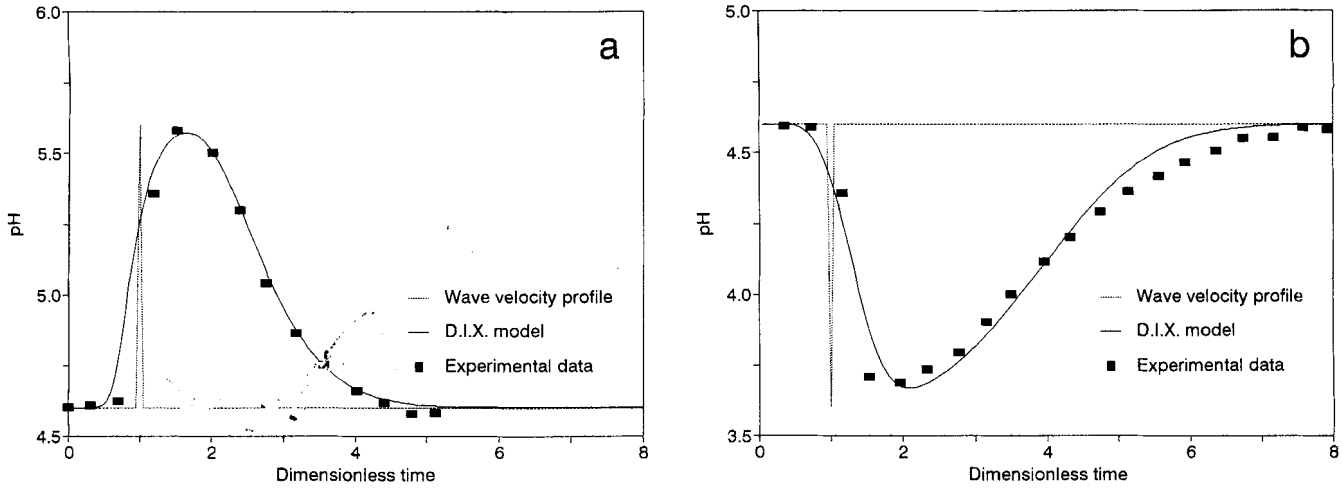

Figure 7. pH response of an Amberlite IRA-400 column to an acetate concentration step change from 0.1 M to 1.0 M at constant feed pH.

(a) Upward concentration step; (b) downward concentration step. Experimental data from Helfferich and Bennett (1984a).

ues were $S_{Na^+,H^+} = 0.10$ and $K^{ov}_{Hac} = 1.52$. In the simulations 20 spatial discretization steps were used. The wave velocity concept, in combination with the premise by Helfferich and Bennett that undissociated acetic acid is not taken up by the resin, fails to describe the pH response correctly. The DIX model, with linear uptake of the neutral species, appears to be well able to describe the column behavior (Figure 7). The model's flexibility in use for different types of resins is supported by these simulations.

Similar concentration step experiments were done in this study with Macro-Prep Q. A column was equilibrated with an acetate solution of 10 mmol/L and a step in the influent concentration to 100 mmol/L was applied, and *vice versa* (Figure 8). Because of the relatively low coion uptake under the applied conditions, the combined Na^+/Ac^- wave, resulting from the increase of the influent concentration, migrates through the column at approximately the mobile phase velocity. Acetate anions are coupled with sodium cations in order to maintain electroneutrality. This wave is accompanied by a pH increase due to the displacement of OH^- on the resin phase by the increased acetate concentration. After the first breakthrough, the total acetate concentration in the effluent is leveled off and the effluent pH remains constant for some time. Then a second wave of undissociated acetic acid, moving at a velocity lower than the liquid phase velocity, appears at the outlet and the effluent concentration and pH proceed to the influent values. The temporary stabilization of the pH is due to the proton redistribution accompanying the uptake or release of undissociated acetic acid. Again the column response is slower and the effect is more lengthy in the least buffered systems. The same principles that apply for the upward concentration step also apply to the reverse step from high to low concentration.

Model simulations with the parameters obtained as shown above described the experimental profiles only qualitatively (Figure 8). The plateau in the measured concentration profile is reduced to a bend in the simulated profile and the plateau in the pH is absent, but the location of the bend in

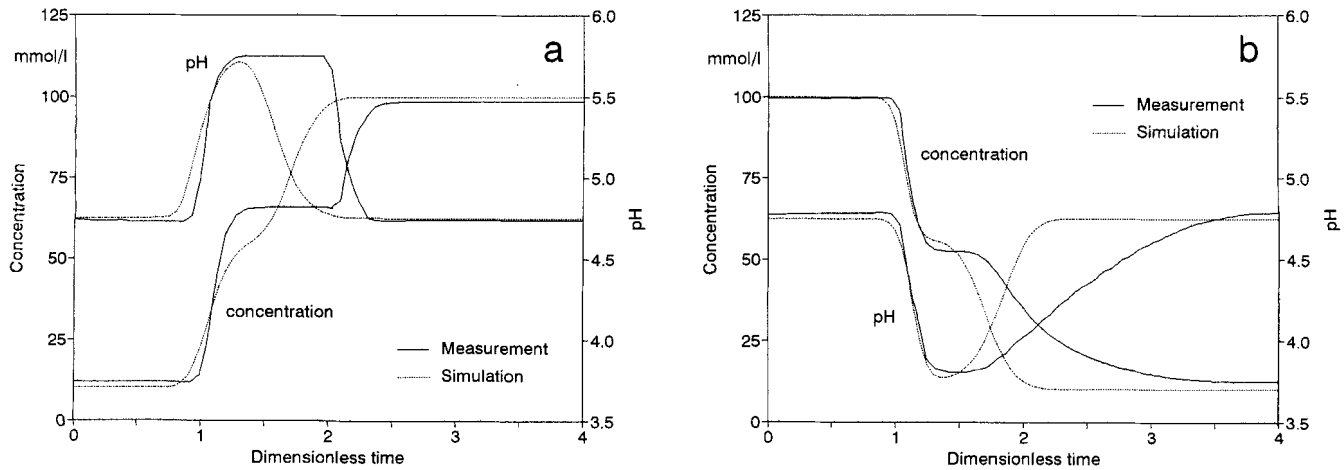

Figure 8. Response of a column equilibrated with an acetate solution of pH 4.75 after a change in the influent concentration (a) from 10 mmol/L to 100 mmol/L and (b) from 100 mmol/L to 10 mmol/L.

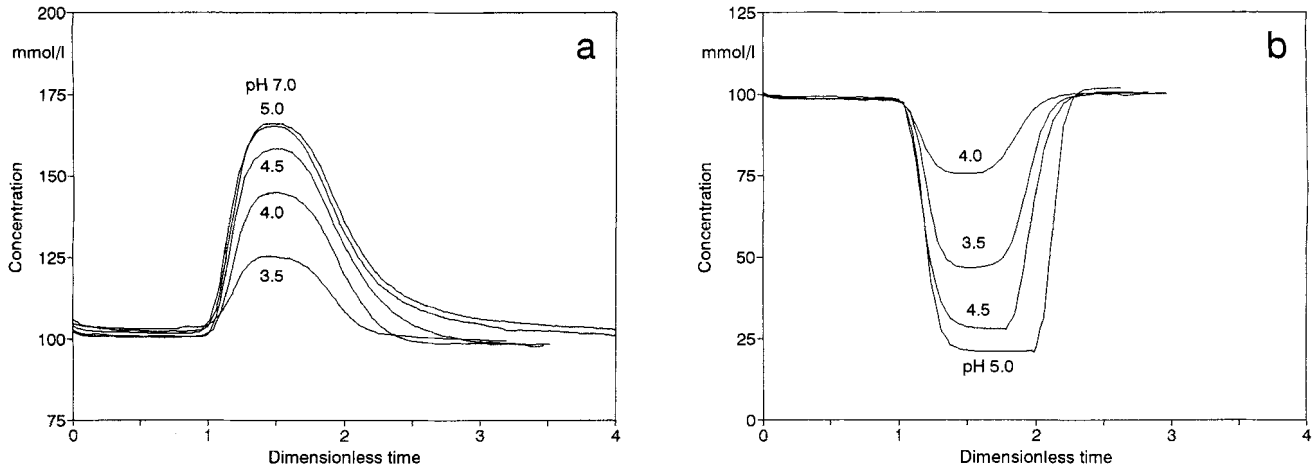

Figure 9. Effluent total *N*-acetylmethionine concentrations in response to block pulses of *N*-acetylmethionine solutions with different pH values at a constant feed concentration of 100 mmol/L.

(a) Block-pulse front; (b) block-pulse tail.

the concentration profile and the maximum of the pH deviation are predicted quite well for both experiments (results for pH 6 are not shown). A better agreement was obtained when a 2–3 times higher value for the distribution coefficient was used in the simulations, but there is no reason to assume that the value of $K^{ov}_{HAc} = 1.079$ is incorrect. Further research is required in order to explain these phenomena more quantitatively.

Block-pulse of pH at fixed N-acetylmethionine concentration

The course of the effluent concentration of a column in equilibrium with 100 mM *N*-acetylmethionine of pH 3.00 to a block-pulse in the pH of the feed is presented in Figure 9 and the pH response is presented in Figure 10. The observed behavior and the underlying mechanisms are very similar to those in comparable experiments with acetic acid.

A difference between *N*-acetylmethionine and acetic acid is that the former is a somewhat stronger acid (*N*-acetylmethionine: $pK_a = 3.54$, acetic acid: $pK_a = 4.76$) (Wandrey and Flaschel, 1979), resulting in a shift of the observed phenomena towards lower pH values. Moreover, *N*-acetylmethionine is amphoteric; at low pH, about 2–3, *N*-acetylmethionine takes up a proton and becomes positively charged. Nevertheless, in the pH range investigated, the occurrence of the *N*-acetylmethionine cation is of minor importance, so only the neutral molecule and anion are considered. As with acetate, the excess uptake of *N*-acetylmethionine is mainly determined by the neutral molecule and the overall distribution coefficient is determined in the same way.

In Figure 11 the excess concentrations are plotted against the concentration of undissociated *N*-acetylmethionine. From the slope of the curve through those data corresponding to pH values below 5.5 a value of $K^{ov}_{AcM} = 1.33$ is obtained. A value of 1.423 is obtained if the data are fitted with the DIX

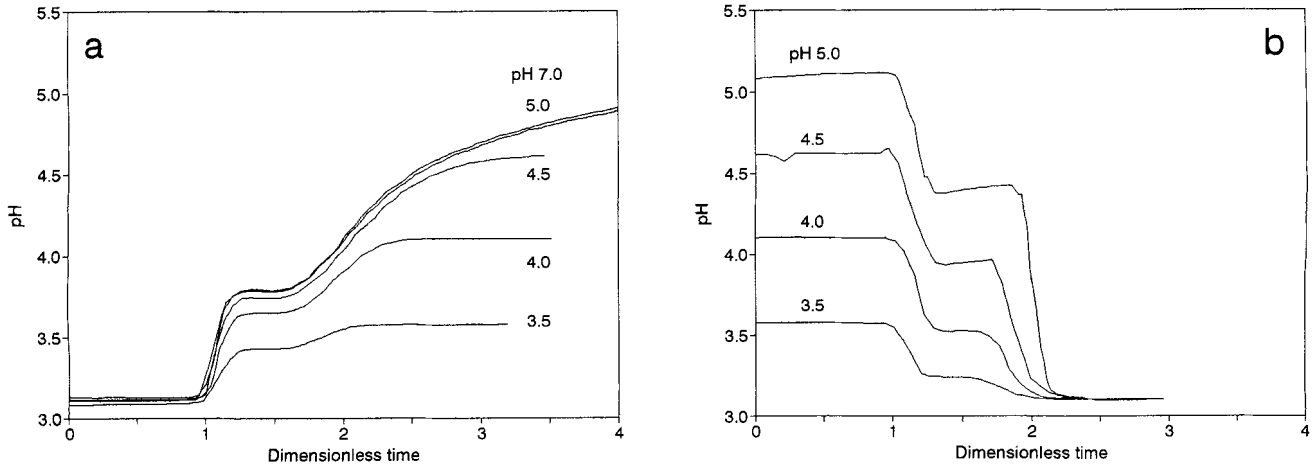

Figure 10. Effluent pH in response to block pulses of *N*-acetylmethionine solutions with different pH values at a constant feed concentration of 100 mmol/L.

(a) Block-pulse front; (b) block-pulse tail.

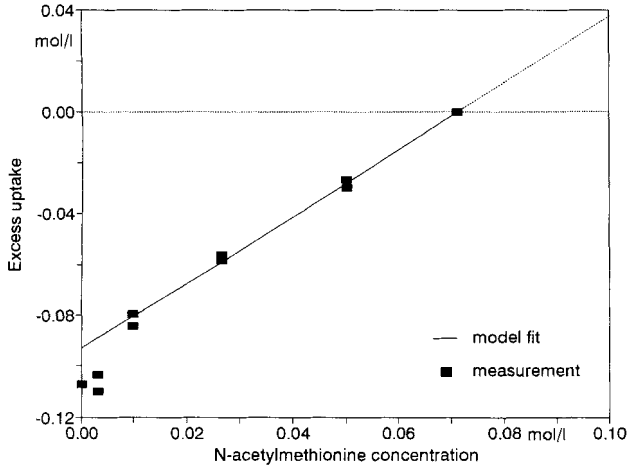

Figure 11. Excess resin phase concentration of *N*-acetylmethionine as a function of the undissociated *N*-acetylmethionine concentration relative to the *N*-acetylmethionine uptake at pH 3.00 at a constant feed concentration of 100 mmol/L.

model, using the following parameters obtained previously from batch equilibrium experiments with *N*-acetylmethionine: $S_{AcM^-,OH^-} = 0.033$, $S_{AcM^+,H^+} = 0.565$ and $S_{Na^+,H^+} = 15.2$ (Jansen et al., 1996a). However, within the specified pH range the model is quite insensitive to changes in these parameter values. Estimation of the distribution coefficient from the position of the second wave, between 1.5 and 2 residence times, gives a value approximately equal to 1.3, which also corresponds well to that of the other methods. The distribution coefficient estimated from batch equilibrium experiments (Jansen et al., 1996a) was 0.85 ± 0.32 mol/L. Correction of this value for the fact that part of the intraparticle water actually belongs to the resin phase gives a value of 1.3, which is also in very good agreement with the other results.

Under the applied conditions the total resin phase concentration of undissociated *N*-acetylmethionine at pH 3.00 is about 0.1 mol/L, which is roughly 30% of the resin capacity. The uptake of undissociated *N*-acetylmethionine may thus contribute significantly to the total uptake of this component, especially at low pH and high liquid phase concentrations. The overall distribution coefficient of undissociated *N*-acetylmethionine is approximately 30% higher than that of acetic acid, but the fraction of undissociated acetic acid is higher than that of neutral *N*-acetylmethionine at each pH due to a lower pK_a value of the latter and its transition to the protonated form at low pH. The net result is that the excess uptake of undissociated species is always in favor of acetate. The actual separation of the two components strongly depends on the pH as well as on the concentration. At low concentrations, the ion-exchange mechanism, and thus the anion fraction, is of major importance (Jansen et al., 1996b) whereas at higher concentration the total uptake, including that of coions and neutral species, is important

Simulation of block-pulse in influent pH with N-acetylmethionine

The response of a block pulse of pH 3.10 to 4.62 and vice versa was measured and simulated (see Figure 12). The parameters used in the simulations were: $S_{Na^+,H^+} = 15.2$, $S_{AcM^+,OH^-} = 0.033$, $S_{AcM^+,H^+} = 0.565$ and $K^{ov}_{AcM} = 1.423$. For both the upward and the downward pH step the simulated profiles correspond well with the experimental profiles, except that the plateaus in the pH are less distinct in the simulations. Adjusting the number of discretization steps to obtain sharper profiles is an option. The number of discretization steps was chosen equal to that used for the acetate experiments, but the required number is in fact component-dependent since the apparent dispersion coefficient is a function of the mass-transfer properties of the species involved (Guiochon et al., 1994; see also the appendix). The success of adjusting the number of discretization steps is however questionable because the first wave and the second wave differ very much in width, but this is not the case in the simulation. Just as in the case of acetate, the best simulation results were obtained in the lower pH region where the buffer capacity of the system is not too low.

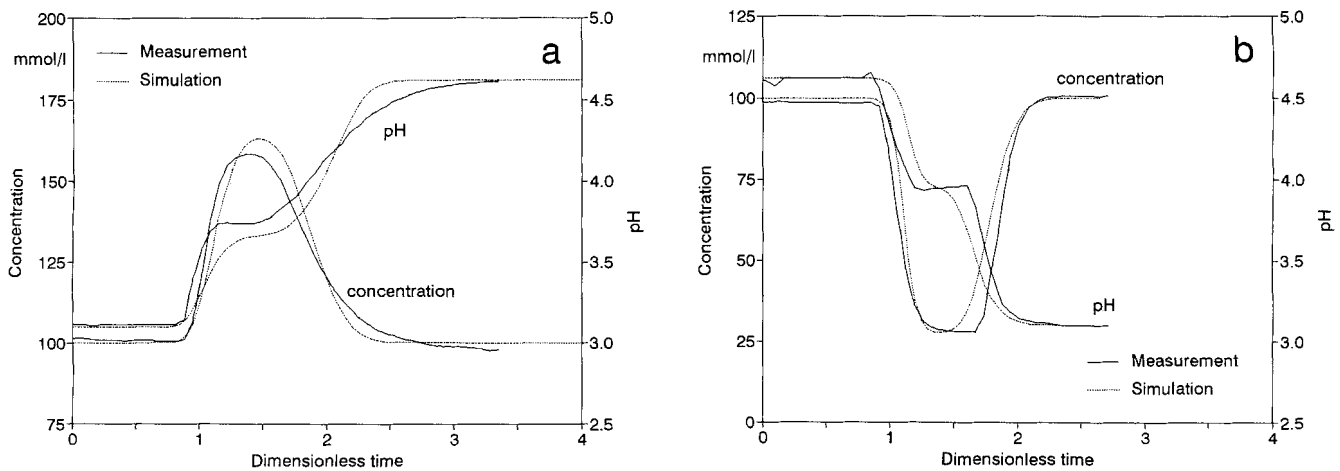

Figure 12. Response of a column in equilibrium with 100 mmol/L *N*-acetylmethionine of pH 3.10 to a block pulse of 100 mmol/L *N*-acetylmethionine of pH 4.62.

(a) Upward pH step; (b) downward pH step.

Evaluation of model and model parameter values

In the foregoing it has been shown that the DIX equilibrium model can be used successfully for the description of the dynamics of the ion exchange of several weak electrolytes on different ion-exchange resins. The contribution to the model of the uptake of undissociated species proved to be an extremely useful extension. Consequently, much better than conventional models, this model is able to describe the behavior of weak electrolyte systems both qualitatively and quantitatively. The significance of coion uptake, by which the DIX model also distinguishes itself from other models, was not studied in detail here.

The deviations between experimental results and simulations that were sometimes found are more likely due to incorrect parameter values than to be caused by errors in the model structure. Several model parameters were determined previously from batch equilibrium experiments but these could not all be determined with great accuracy, in particular the bed porosity and the overall distribution coefficients for neutral species. The alternative parameter estimation methods discussed in this article lead to results that are in general in good quantitative agreement with the previously obtained results. The wave velocity concept is very helpful in explaining the dynamic behavior of the simple weak electrolyte systems investigated in this study. The fixed-bed model based on the DIX equilibrium model described most of the experiments well and appears to be adequate, except for moderately buffered systems. Lumping all dispersive, kinetic and mass-transfer effects into a single parameter is probably an oversimplification for situations where very small quantities of a component play an important role through the influence on the pH of the system. This requires more attention in the future.

Under the conditions of this study, the model was found to be quite insensitive to the values of the selectivities obtained from batch equilibrium experiments. The number of parameters is also quite large. Depending on the conditions, some of the parameters can possibly be omitted and the model be simplified in future applications if the sensitivity of the model to certain parameters is very low. Conversely, parameter values for K_i^{ov} and ϵ_b, as obtained in this study, can be used for the description of the batch experiments. This is not likely to yield new information since the values found in this study lie well within the error margins of the batch parameters.

Conclusions

The experiments described in this article unarguably demonstrate the importance of the often neglected uptake of undissociated species in ion exchangers. From weak electrolyte solutions with concentrations of about one-third of the capacity of the resin, quantities of neutral species corresponding to 30% of the capacity are taken up. This contribution is expected to be proportionally higher at higher concentrations and even become dominant in overload situations.

The complex column dynamics of ion-exchange processes of several weak electrolytes and different resins were for the greater part described correctly with fixed-bed model based on the Donnan Ion eXchange equilibrium model. Conventional models are less successful in predicting pH and concentration responses of the effluent to disturbances in the feed. Incorporating the uptake of coions and especially that of neutral species is a major improvement compared to conventional models. Application of the wave velocity concept was very helpful for a qualitative as well as quantitative explanation of the results. But unlike in Helfferich's approach (Helfferich and Bennett, 1984a) acetic acid and acetate were treated as distinct species, each with its own wave, although the acetate wave was a combined wave with sodium. Also for *N*-acetylmethionine, a distinction was made between the different ionic forms. The wave velocity concept can thus be applied successfully to weak electrolyte systems provided that the system is defined correctly and all participating species are identified, following Klein (1981).

This study of single component systems has contributed to a better understanding of the factors playing a role in the column dynamics of ion-exchange processes involving weak electrolytes. The same factors are important for multicomponent systems in general and for chromatographic separation of (weak) electrolyte mixtures in particular. Especially the pH, because of its influence on the ionic forms in which components occur, is of primary importance and can be exploited to accomplish separation of weak electrolytes. More attention is paid to the pH in subsequent work where more-component systems are investigated (Jansen et al., 1996b). Simulations with the fixed-bed model will be very helpful in describing column dynamics and in finding the optimal conditions required for separation processes of weak electrolyte mixtures.

Acknowledgment

HPLC Analyses were done by C. Ras, whose effort and contribution to this study are gratefully acknowledged. The authors also wish to thank Dr. D. M. F. T. dos Prazeres for the explorative investigations, Dr. J. C. Bellot for the many discussions on ion-exchange chromatography and J. J. M. Potters for his comments on the characteristic times concept.

Literature Cited

Bellot, J. C., and J. S. Condoret, "Liquid Chromatography Modelling: A Review," *Process Biochem.*, **26**, 363 (1991).

Bennett, B. J., and F. G. Helfferich, "pH Waves in Anion Exchange Columns," *Ion Exchange Technology*, D. Naden and M. Streat, eds., Ellis Horwood, Chichester, U.K., p. 322 (1984).

Bio-Rad, "New Macro-Prep™ 50Q, S, and CM Ion Exchange Supports," Bulletin 1623, Bio-Rad, Richmond (1990).

Carta, G., M. S. Saunders, J. P. DeCarli II, and J. B. Vierow, "Dynamics of Fixed-Bed Separations of Amino Acids by Ion-Exchange," *AIChE Symp. Ser.*, **84(264)**, 54 (1988).

Chibata, I., and T. Tosa, "Industrial Applications of Immobilized Enzymes and Immobilized Microbial Cells," *Applied Biochemistry and Bioengineering: 1. Immobilized Enzyme Principles*, L. B. Wingard, E. Katchalski-Katzir, and L. Goldstein, eds., Academic Press, New York, p. 329 (1976).

DeCarli, J. P. II, G. Carta, and C. H. Byers, "Displacement Separations by Continuous Annular Chromatography," *AIChE J.*, **36(8)**, 1220 (1990).

Golshan-Shirazi, S., and G. Guiochon, "The Equilibrium-Dispersive Model of Chromatography," *Theoretical Advancement in Chromatography and Related Separation Techniques, NATO ASI Series C*, F. Dondi and G. Guiochon, eds., Kluwer Academic Publishers, Dordrecht, Vol. 383, p. 35 (1992).

Guiochon, G., S. Golshan Shirazi, and A. M. Katti, *Fundamentals of Preparative and Nonlinear Chromatography*, Academic Press, Boston, Chaps. II, VI, X, XI (1994).

Harland, C. E., *Ion Exchange. Theory and Practice*, 2nd ed., Ch. 6, Roy. Soc. of Chemistry, Cambridge (1994).

Helfferich, F. G., *Ion Exchange*, McGraw-Hill, New York, p. 95 (1962).

Helfferich, F. G., "Ion-Exchange Equilibria of Amino Acids on Strong-Acid Resins: Theory," *React. Poly.*, **12**, 95 (1990).
Helfferich, F. G., and B. J. Bennett, "Weak Electrolytes, Polybasic Acids, and Buffers in Anion Exchange Columns I. Sodium Acetate and Sodium Carbonate Systems," *React. Poly.*, **3**, 51 (1984a).
Helfferich, F. G., and B. J. Bennett, "Weak Electrolytes, Polybasic Acids, and Buffers in Anion Exchange Columns II. Sodium Acetate Chloride Systems," *Solvent Extr. Ion Exch.*, **2(7–8)**, 1151 (1984b).
Jansen, M. L., A. J. J. Straathof, L. A. M. van der Wielen, K. Ch. A. M. Luyben, and W. J. J. van den Tweel, "Rigorous Model for Ion Exchange Equilibria of Strong and Weak Electrolytes," *AIChE J.*, **42**, 1911 (1996a).
Jansen, M. L., J. Houwers, A. J. J. Straathof, L. A. M. van der Wielen, K. Ch. A. M. Luyben, and W. J. J. van den Tweel, "Influence of Secondary Equilibria on Ion-Exchange Processes of Weak Electrolytes: The Effect of Dissociation Reactions," *AIChE J.*, submitted (1996b).
Jones, I. L., and G. Carta, "Ion Exchange of Amino Acids and Dipeptides on Cation Resins with Varying Degree of Cross-Linking: 1. Equilibrium," *Ind. Eng. Chem. Res.*, **32**, 107 (1993a).
Jones, I. L., and G. Carta, "Ion Exchange of Amino Acids and Dipeptides on Cation Resins with Varying Degree of Cross-Linking: 2. Intraparticle Transport," *Ind. Eng. Chem. Res.*, **32**, 117 (1993b).
Kawakita, T., and T. Matsuishi, "Elution Kinetics of Lysine from a Strong Cation-Exchange Resin with Ammonia Water," *Sep. Sci. Technol.*, **26(7)**, 991 (1991).
Klein, G., "Ion Exchange and Chemical Reaction in Fixed Beds," *Percolation Processes: Theory and Applications*, A. E. Rodrigues and D. Tondeur, eds., Sijthoff & Noordhoff, Alphen aan den Rijn, p. 363 (1981).
Mehablia, M. A., D. C. Shallcross, and G. W. Stevens, "Prediction of Multicomponent Ion Exchange Equilibria," *Chem. Eng. Sci.*, **49**, 2277 (1994).
Myers, A. L., and S. Byington, "Thermodynamics of Ion Exchange: Prediction of Multicomponent Equilibria from Binary Data," *Ion Exchange Technology*, A. E. Rodrigues, ed., Nijhoff, Dordrecht, The Netherlands, p. 119 (1986).
Reichenberg, D., and W. F. Wall, "The Absorption of Uncharged Molecules by Ion-Exchange Resins," *J. Chem. Soc.*, 3364 (1956).
Saunders, M. S., J. B. Vierow, and G. Carta, "Uptake of Phenylalanine and Tyrosine by a Strong-Acid Cation Exchanger," *AIChE J.*, **35(1)**, 53 (1989).
Wandrey, C., and E. Flaschel, "Process Development and Economic Aspects in Enzyme Engineering. Acylase L-methionine System," *Adv. Biochem. Eng.*, **12**, 147 (1979).
Wielen, L. A. M. van der, A. J. J. Straathof, and K. Ch. A. M. Luyben, "Adsorptive and Chromatographic Bioreactors," *Precision Process Technology*, M. P. C. Weijnen and A. A. H. Drinkenburg, eds., Kluwer Academic Publishers, Dordrecht, The Netherlands, p. 353 (1993).
Wilke, C. R., and P. Chang, "Correlation of Diffusion Coefficients in Dilute Solutions," *AIChE J.*, **1**, 264 (1955).
Yu, Q., J. Yang, and N.-H. L. Wang, "Multicomponent Ion-Exchange Chromatography for Separating Amino Acid Mixtures," *React. Poly.*, **6**, 33 (1987).

Appendix: Analysis of Characteristic Times

The local equilibrium assumption in the fixed-bed model can be verified by analysis of characteristic times. Because the ion-exchange process is treated here as a phase equilibrium process rather than as a kinetic process, the relevant subprocesses concern only mass transport: convection and dispersion, external mass transfer and intraparticle diffusion.

The characteristic time for convective transport t_{conv} which is a measure for the time that a liquid element is in contact with the resin, depends on the length of the flow path around a particle, the liquid velocity, and the number of particles contacted by the flowing liquid element

$$t_{conv} = \frac{3}{2}\frac{\epsilon_b \pi d_p}{u_0} \tag{A-1}$$

Here d_p is the particle diameter (m), ϵ_b is the void fraction of the bed, and u_0 is the superficial liquid velocity. The Peclet number in Eq. 8 is a measure for the ratio between the rates of convective and dispersive mass transport, or the inverse ratio between the characteristic times. The Peclet number may be computed from the following relation for axial dispersion in fixed beds (Guiochon et al., 1994)

$$Pe = \frac{L}{\epsilon_b d_p}(0.2 + 0.011\, Re^{0.48}) \tag{A-2}$$

The Reynolds number is defined as $Re = \rho u_0 d_p/\eta$, where ρ is the liquid density ($kg \cdot m^{-3}$) and η the dynamic viscosity (Pa·s). The characteristic time (s) for axial dispersion t_{ax} is thus defined as follows

$$t_{ax} = t_{conv} Pe = \frac{3}{2}\frac{\pi L}{u_0}(0.2 + 0.011\, Re^{0.48}) \tag{A-3}$$

The characteristic time for external mass transfer is determined by the rate of film diffusion and the particle surface. For flow around particles in a packed bed at $0.0015 < Re < 55$, which is usually the case for chromatographic processes, the following relation for the Sherwood number Sh is given by Guiochon et al. (1994)

$$Sh = \frac{k_L d_p}{D_L} = \frac{1.09}{\epsilon_b} Re^{\frac{1}{3}} Sc^{\frac{1}{3}} \tag{A-4}$$

With k_L the liquid phase mass-transfer coefficient ($m \cdot s^{-1}$), D_L the liquid phase diffusion coefficient and Sc the Schmidt number $Sc = \eta/\rho D_L$. For spherical particles the surface per volume of liquid a ($m^2 \cdot m^{-3}$) is equal to $6(1-\epsilon_b)/\epsilon_b d_p$. The characteristic time for external mass transfer t_{film} is equal to $1/k_L a$. Substitution into Eq. A-4 gives

$$t_{film} = 0.153 \frac{\epsilon_b^2 d_p^2}{(1-\epsilon_b) D_L} Re^{-\frac{1}{3}} Sc^{-\frac{1}{3}} \tag{A-5}$$

The characteristic time for intraparticle diffusion t_{diff} is determined by the diffusion path (particle radius) and the effective diffusion coefficient for the resin phase D_R with a correction factor for the spherical geometry. From the solution of the mass balance for penetration into a spherical particle (Harland, 1994) the following expression results

$$t_{diff} = \frac{d_p^2}{4\pi^2 D_R} \tag{A-6}$$

The magnitude of the diffusion coefficient of component i in solvent s can be estimated using the relation by Wilke and Chang (1955)

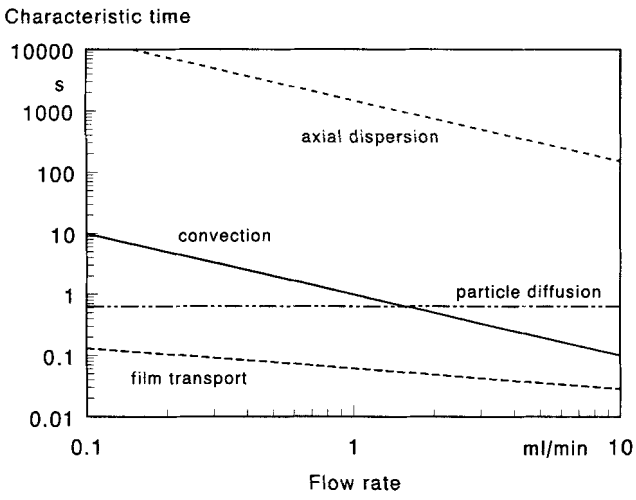

Figure 13. Calculated characteristic times for convective mass transport, axial dispersion, external mass transfer, and intraparticle diffusion as function of the flow rate.

Column diameter, 0.015 m; column length, 0.15 m; particle diameter, 50 μm; diffusion coefficient liquid, 10^{-9} m^2/s; diffusion coefficient resin, 0.1×10^{-9} m^2/s; dynamic viscosity, 10^{-3} Pa·s; bed void fraction, 40%.

$$D_{i,L} = 5.88\times10^{-17}\frac{(\chi_s M_s)^{\frac{1}{2}}T}{\eta v_i^{0.6}} \qquad \text{(A-7)}$$

Here χ is an association parameter (2.6 for water), M_s is the molar mass of the solvent (kg·mol^{-1}), T the temperature (K) and v_i the molar volume of the solute at its boiling point. From this equation a diffusion coefficient for acetate in water of 1.3×10^{-9} m^2/s can be calculated, for methionine the value is approximately 0.9×10^{-9} m^2/s and for *N*-acetylmethionine 0.75×10^{-9} m^2/s. The diffusion coefficient in the resin phase can be related to the liquid-phase diffusion coefficient using the following empirical relation (Harland, 1994; Guiochon et al., 1994)

$$D_R = D_L\left(\frac{\epsilon_p}{2-\epsilon_p}\right)^2 \qquad \text{(A-8)}$$

in which ϵ_p is the intraparticle void fraction, which is approximately 75% for the resin under consideration, giving a diffusivity ratio of 0.36 between resin and liquid phase. Jones and Carta (1993b) have also derived an empirical relation between resin and liquid-phase diffusivities for various amino acids and dipeptides in cation-exchange resins and predict diffusivity ratios between 0.1 and 0.001. Considering this, the resin phase diffusion coefficient was estimated to be 0.1×10^{-9} m^2/s. The dynamic viscosity was assumed to be equal to that of water, 10^{-3} Pa·s. The ion-exchange resin used in the present study Macro-Prep Q has an average particle diameter of 50 μm (Bio-Rad, 1990). The column experiments were carried out using a column with an internal diameter of 1.5 cm, a bed length of approximately 15 cm, and a flow rate in the order of magnitude of 5 mL/min. The void fraction in the bed with uniform spherical particles is about 40%. Using these data, the characteristic times were calculated and the results are plotted in Figure 13.

In the entire range of flow rates the Peclet number is approximately 1,500. Hence, mass transport by axial dispersion is negligible compared to convective mass transport. At low flow rates, the characteristic time for mass transport by convection is larger than those for diffusion so the assumption of local equilibrium is justified. Going to higher flow rates, intraparticle diffusion becomes increasingly important. In the range of flow rates that is of interest for the present study, the characteristic time for diffusion and that for convection have the same order of magnitude and therefore the local equilibrium assumption must be used with caution. Due to these mass-transfer effects, additional dispersion is likely to occur in the ion-exchange column. In the dynamic chromatography model the actual dispersion should be replaced by numerical dispersion by choosing the right number of space and time discretization steps. This can be done by calculating the step size from the apparent dispersion coefficient, if known (Guiochon et al., 1994), or by adjusting the step size until a reasonable fit to the experimental curves is obtained (Carta et al., 1988). The latter method was applied in this article.

Manuscript received July 17, 1995, and revision received Oct. 30, 1995.